On the precision of a data-driven estimate of hadronic light-by-light scattering in the muon $g-2$: pseudoscalar-pole contribution

Andreas Nyffeler

Institut für Kernphysik

Johannes Gutenberg Universität Mainz, Germany

nyffeler@kph.uni-mainz.de

Working Group on Radiative Corrections and Generators for Low Energy Hadronic Cross Section and Luminosity
LNF, Frascati, Italy
19-20 May 2016

JG|U JOHANNES GUTENBERG UNIVERSITÄT MAINZ

SFB 1044 THE LOW-ENERGY FRONTIER OF THE STANDARD MODEL

Outline

- Introduction: current status of muon $g-2$ and hadronic light-by-light scattering (HLbL)
- Data-driven approach to HLbL using dispersion relations
- Pseudoscalar-pole contribution: 3-dim. integral representation
- Model independent weight functions for $\mathrm{P} = \pi^0, \eta, \eta'$
- Relevant momentum regions in $a_\mu^{\mathrm{HLbL;P}}$
- Impact of form factor uncertainties on $a_\mu^{\mathrm{HLbL;P}}$
- Conclusions and Outlook

Muon $g-2$: current status

Contribution	$a_\mu \times 10^{11}$	Reference
QED (leptons)	116 584 718.853 $\pm$ 0.036	Aoyama et al. '12
Electroweak	153.6 $\pm$ 1.0	Gnendiger et al. '13
HVP: LO	6889.1 $\pm$ 35.2	Jegerlehner '15
NLO	-99.2 $\pm$ 1.0	Jegerlehner '15
NNLO	12.4 $\pm$ 0.1	Kurz et al. '14
HLbL	116 $\pm$ 39	Jegerlehner, AN '09
NLO	3 $\pm$ 2	Colangelo et al. '14
Theory (SM)	116 591 794 $\pm$ 53	
Experiment	116 592 089 $\pm$ 63	Bennett et al. '06
Experiment - Theory	295 $\pm$ 82	3.6 σ

HVP: Hadronic vacuum polarization
HLbL: Hadronic light-by-light scattering

Other estimates: $\sim (3-5)\ \sigma$ deviation.
Discrepancy a sign of New Physics ? Hadronic uncertainties need to be better controlled in order to fully profit from future $g-2$ experiments with $\delta a_\mu = 16 \times 10^{-11}$. Way forward for HVP seems clear with more precise measurements for $\sigma(e^+e^- \to \text{hadrons})$, not so obvious how to improve HLbL.

HLbL in muon $g-2$

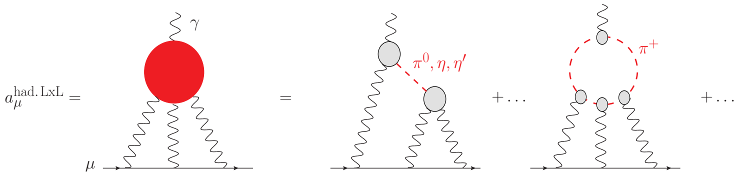

- Only model calculations so far: large uncertainties, difficult to control.
- Frequently used estimates:

$$a_\mu^{\mathrm{HLbL}} = (105 \pm 26) \times 10^{-11}$$ (Prades, de Rafael, Vainshtein '09) ("Glasgow consensus")

$$a_\mu^{\mathrm{HLbL}} = (116 \pm 39) \times 10^{-11}$$ (AN '09; Jegerlehner, AN '09)

Based almost on same input: calculations by various groups using different models for individual contributions. Error estimates are mostly guesses !

HLbL: recent developments

- Need much better understanding of complicated hadronic dynamics to get reliable error estimate of $\pm 20 \times 10^{-11}$ ($\sim 20\%$) (or even 10%).
- Recent new proposal: Colangelo et al. '14, '15; Pauk, Vanderhaeghen '14: use dispersion relations (DR) to connect contribution to HLbL from light pseudoscalars to, in principle, measurable form factors and cross-sections with two off-shell photons:

$$\gamma^*\gamma^* \quad \to \quad \pi^0, \eta, \eta'$$
$$\gamma^*\gamma^* \quad \to \quad \pi^+\pi^-, \pi^0\pi^0$$

  Could connect HLbL uncertainty to experimental measurement errors, like HVP. Note: no data yet with two off-shell photons !

- Future: HLbL from Lattice QCD.
  First steps: Blum et al. '05, ..., '14, '15.
  Work started by Lattice group in Mainz (Green et al. '15).

Data-driven approach to HLbL using dispersion relations (DR)

Strategy: Split contributions to HLbL into two parts:

I: Data-driven evaluation using DR (hopefully numerically dominant):

- (1) π^0, η, η' poles
- (2) $\pi\pi$ intermediate state

II: Model dependent evaluation (hopefully numerically subdominant):

- (1) Axial vectors (3π-intermediate state), ...
- (2) Quark-loop, matching with pQCD

Error goals: Part I: 10% precision (data driven), Part II: 30% precision.
To achieve overall error of about 20% ($\delta a_\mu^{\text{HLbL}} = 20 \times 10^{-11}$).

Colangelo et al.:
Classify intermediate states in 4-point function. Then project onto $g - 2$.

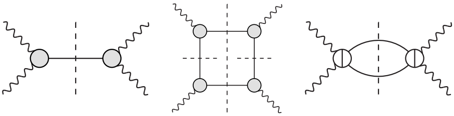

Pauk, Vanderhaeghen:
Write DR directly for Pauli form factor $F_2(k^2)$.

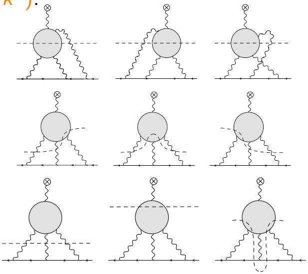

Pseudoscalar contribution to HLbL

- Most calculations for neutral pion and all light pseudoscalars π^0, η, η' agree at level of 15%, but full range of estimates (central values) much larger:

$$a_\mu^{\mathrm{HLbL};\pi^0} = (50 - 80) \times 10^{-11} = (65 \pm 15) \times 10^{-11} \ (\pm 23\%)$$

$$a_\mu^{\mathrm{HLbL;P}} = (59 - 114) \times 10^{-11} = (87 \pm 27) \times 10^{-11} \ (\pm 31\%)$$

- This talk: study precision which could be reached with data-driven estimate of pseudoscalar-pole contribution to HLbL (AN, arXiv:1602.03398 [hep-ph]).

- Relevant momentum regions where data on doubly off-shell transition form factor $\mathcal{F}_{\mathrm{P}\gamma^*\gamma^*}(-Q_1^2, -Q_2^2)$ will be needed from direct experimental measurements, via DR for form factor itself or from Lattice QCD, to better control this numerically dominant contribution to HLbL and its uncertainty.

- Impact on precision of $a_\mu^{\mathrm{HLbL;P}}$ based on estimated experimental uncertainties of $\mathcal{F}_{\mathrm{P}\gamma^*\gamma^*}(-Q_1^2, -Q_2^2)$ using results from Monte Carlo simulation for BESIII (Mainz group: Denig, Redmer, Wasser).

Pion-pole contribution (analogously for η, η') (Knecht, AN '02)

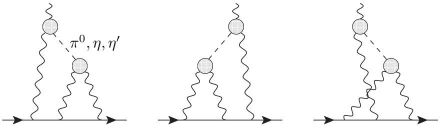

$$a_\mu^{\mathrm{HLbL};\pi^0} = \left(\frac{\alpha}{\pi}\right)^3 \left[a_\mu^{\mathrm{HLbL};\pi^0(1)} + a_\mu^{\mathrm{HLbL};\pi^0(2)}\right]$$

$$a_\mu^{\mathrm{HLbL};\pi^0(1)} = \int \frac{d^4 q_1}{(2\pi)^4} \frac{d^4 q_2}{(2\pi)^4} \frac{1}{q_1^2 q_2^2 (q_1+q_2)^2 [(p+q_1)^2 - m_\mu^2][(p-q_2)^2 - m_\mu^2]} \times \frac{\mathcal{F}_{\pi^0\gamma^*\gamma^*}(q_1^2, (q_1+q_2)^2) \; \mathcal{F}_{\pi^0\gamma^*\gamma^*}(q_2^2, 0)}{q_2^2 - m_\pi^2} \; \tilde{T}_1(q_1, q_2; p)$$

$$a_\mu^{\mathrm{HLbL};\pi^0(2)} = \int \frac{d^4 q_1}{(2\pi)^4} \frac{d^4 q_2}{(2\pi)^4} \frac{1}{q_1^2 q_2^2 (q_1+q_2)^2 [(p+q_1)^2 - m_\mu^2][(p-q_2)^2 - m_\mu^2]} \times \frac{\mathcal{F}_{\pi^0\gamma^*\gamma^*}(q_1^2, q_2^2) \; \mathcal{F}_{\pi^0\gamma^*\gamma^*}((q_1+q_2)^2, 0)}{(q_1+q_2)^2 - m_\pi^2} \; \tilde{T}_2(q_1, q_2; p)$$

where $p^2 = m_\mu^2$ and the external photon has now zero four-momentum (soft photon).

Pion-pole contribution determined by measurable pion transition form factor (TFF) $\mathcal{F}_{\pi^0\gamma^*\gamma^*}(q_1^2, q_2^2)$ (on-shell pion, one or two off-shell photons).

Currently, only single-virtual TFF $\mathcal{F}_{\pi^0\gamma^*\gamma^*}(-q^2, 0)$ has been measured (mostly) for spacelike momenta.

η, η': for single-virtual TFF also timelike data from single Dalitz decays.

3-dimensional integral representation (Jegerlehner, AN '09)

$$a_\mu^{\mathrm{HLbL};\pi^0} = \left(\frac{\alpha}{\pi}\right)^3 \left[a_\mu^{\mathrm{HLbL};\pi^0(1)} + a_\mu^{\mathrm{HLbL};\pi^0(2)}\right]$$

$$a_\mu^{\mathrm{HLbL};\pi^0(1)} = \int_0^\infty dQ_1 \int_0^\infty dQ_2 \int_{-1}^1 d\tau\, w_1(Q_1, Q_2, \tau) \mathcal{F}_{\pi^0\gamma^*\gamma^*}(-Q_1^2, -(Q_1+Q_2)^2) \mathcal{F}_{\pi^0\gamma^*\gamma^*}(-Q_2^2, 0)$$

$$a_\mu^{\mathrm{HLbL};\pi^0(2)} = \int_0^\infty dQ_1 \int_0^\infty dQ_2 \int_{-1}^1 d\tau\, w_2(Q_1, Q_2, \tau) \mathcal{F}_{\pi^0\gamma^*\gamma^*}(-Q_1^2, -Q_2^2) \mathcal{F}_{\pi^0\gamma^*\gamma^*}(-(Q_1+Q_2)^2, 0)$$

$$w_1(Q_1, Q_2, \tau) = \left(-\frac{2\pi}{3}\right) \sqrt{1-\tau^2}\, \frac{Q_1^3 Q_2^3}{Q_2^2 + m_\pi^2}\, I_1(Q_1, Q_2, \tau)$$

$$w_2(Q_1, Q_2, \tau) = \left(-\frac{2\pi}{3}\right) \sqrt{1-\tau^2}\, \frac{Q_1^3 Q_2^3}{(Q_1 + Q_2)^2 + m_\pi^2}\, I_2(Q_1, Q_2, \tau)$$

- After Wick rotation: Q_1, Q_2 are Euclidean (spacelike) four-momenta. Integrals run over the lengths of the four-vectors with $Q_i \equiv |(Q_i)_\mu|, i = 1, 2$ and angle θ between them: $Q_1 \cdot Q_2 = Q_1 Q_2 \cos\theta,\ \tau = \cos\theta$.
- Separation of generic kinematics described by model-independent weight functions $w_{1,2}(Q_1, Q_2, \tau)$ and double-virtual form factors $\mathcal{F}_{\pi^0\gamma^*\gamma^*}(-Q_1^2, -Q_2^2)$ which can in principle be measured.
- $w_{1,2}(Q_1, Q_2, \tau)$: dimensionless. $w_2(Q_1, Q_2, \tau)$ symmetric under $Q_1 \leftrightarrow Q_2$.
- $w_{1,2}(Q_1, Q_2, \tau) \to 0$ for $Q_{1,2} \to 0$. $w_{1,2}(Q_1, Q_2, \tau) \to 0$ for $\tau \to \pm 1$.

Model independent weight functions for π^0, η, η'

Weight function $w_1(Q_1, Q_2, \tau)$ for π^0

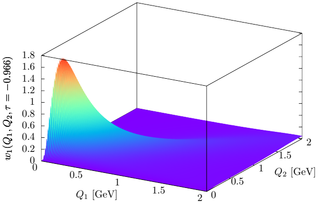

$\tau = -0.966, \quad \theta = 165^\circ$

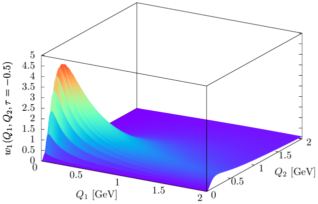

$\tau = -0.5, \quad \theta = 120^\circ$

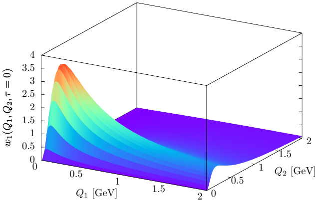

$\tau = 0, \quad \theta = 90^\circ$

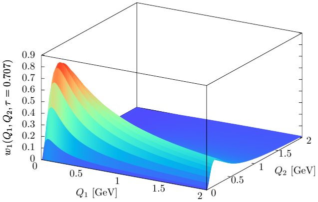

$\tau = 0.707, \quad \theta = 45^\circ$

Low momentum region most important. Peak around $Q_1 \sim 0.2$ GeV, $Q_2 \sim 0.15$ GeV.
Slopes along the two axis and along the diagonal (at $Q_1 = Q_2 = 0$) vanish.
For $\tau > -0.85$ ($\theta < 150^\circ$) a ridge develops along Q_1 direction for $Q_2 \sim 0.2$ GeV.
Leads for constant form factor to a divergence $\ln^2 \Lambda$ for some momentum cutoff Λ.
Realistic form factor falls off for large Q_i and integral $a_\mu^{\mathrm{HLbL};\pi^0(1)}$ will be convergent.

Weight function $w_2(Q_1, Q_2, \tau)$ for π^0

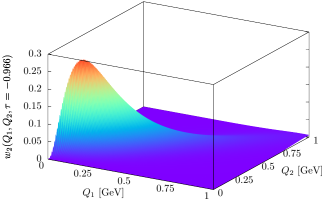

$\tau = -0.966, \quad \theta = 165^\circ$

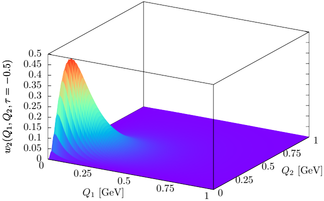

$\tau = -0.5, \quad \theta = 120^\circ$

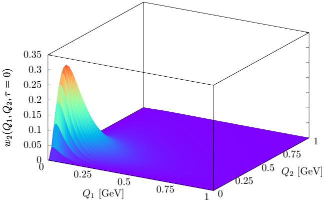

$\tau = 0, \quad \theta = 90^\circ$

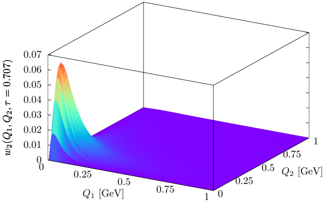

$\tau = 0.707, \quad \theta = 45^\circ$

w_2 about a factor 10 smaller than w_1.
No ridge in one direction, since $w_2(Q_1, Q_2, \tau)$ is symmetric under $Q_1 \leftrightarrow Q_2$.
Peak for $Q_1 = Q_2 \sim 0.15$ GeV for τ near -1, peak moves to lower values $Q_1 = Q_2 = 0.04$ GeV for τ near 1.
Slopes along the two axis and along the diagonal (at $Q_1 = Q_2 = 0$) vanish.
Even for constant form factor, one obtains finite result: $\left(\frac{\alpha}{\pi}\right)^3 a_{\mu;\mathrm{WZW}}^{\mathrm{HLbL};\pi^0(2)} \sim 2.5 \times 10^{-11}$

Variation of $w_{1,2}(Q_1, Q_2, \tau)$ for π^0 with $\tau = \cos\theta$ for selected Q_1, Q_2

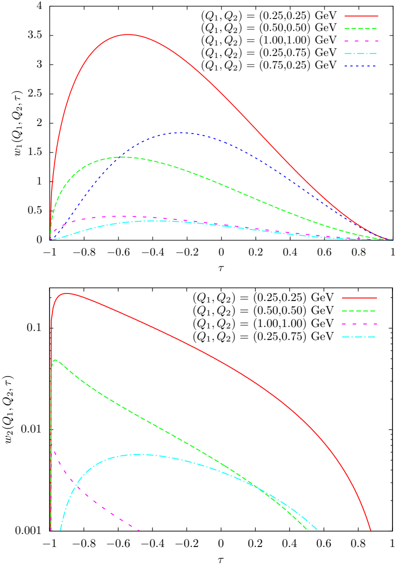

Strong enhancement for $Q_1 = Q_2$ for negative τ, when the original four-vectors $(Q_1)_\mu$ and $(Q_2)_\mu$ become more antiparallel. For $Q_1 = Q_2$ both weight functions have infinite slope at $\tau = -1$. Overall, weight functions get smaller for larger $Q_i > 0.5$ GeV.

Pole contributions from η and η'

Only dependence on pseudoscalars appears in weight functions through pseudoscalar mass m_P in propagators:

$$\text{In weight function } w_1(Q_1, Q_1, \tau): \frac{1}{Q_2^2 + m_P^2}$$

$$\text{In weight function } w_2(Q_1, Q_1, \tau): \frac{1}{(Q_1 + Q_2)^2 + m_P^2} = \frac{1}{Q_1^2 + 2Q_1 Q_2 \tau + Q_2^2 + m_P^2}$$

Two effects:

1. Shifts the relevant momentum regions (peaks, ridges) to higher momenta for η compared to π^0 and even higher for η'.

2. Leads to suppression in absolute size of the weight functions due to larger masses in the propagators. For the bulk of the weight functions we have the approximate relations (at same θ, not necessarily at same momenta):

$$w_1|_\eta \approx \frac{1}{6} \, w_1|_{\pi^0}$$

$$w_1|_{\eta'} \approx \frac{1}{2.5} \, w_1|_\eta$$

Weight functions for η

Weight function $w_1(Q_1, Q_2, \tau)$

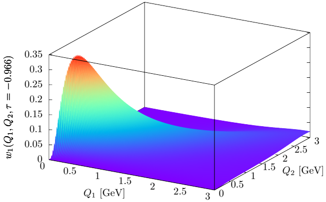

$\tau = -0.966, \quad \theta = 165^\circ$

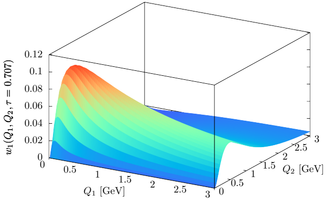

$\tau = 0.707, \quad \theta = 45^\circ$

Weight function $w_2(Q_1, Q_2, \tau)$

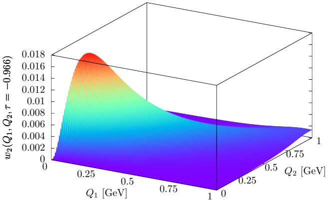

$\tau = -0.966, \quad \theta = 165^\circ$

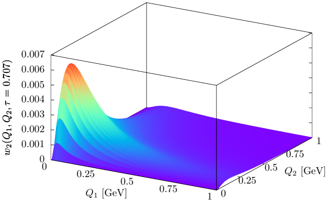

$\tau = 0.707, \quad \theta = 45^\circ$

Peaks and ridges broadened compared to π^0.

Peak for w_1 around $Q_1 \sim 0.32 - 0.37$ GeV, $Q_2 \sim 0.22 - 0.33$ GeV.

w_2 about a factor 20 smaller than w_1. Peak for w_2 around $Q_1 = Q_2 \sim 0.14$ GeV for τ near -1, moves down to $Q_1 = Q_2 = 0.06$ GeV for τ near 1.

w_2: finite result for constant form factor $\left(\frac{\alpha}{\pi}\right)^3 a_{\mu;\mathrm{WZW}}^{\mathrm{HLbL};\eta(2)} = 0.78 \times 10^{-11}$

Weight functions for η'

Weight function $w_1(Q_1, Q_2, \tau)$

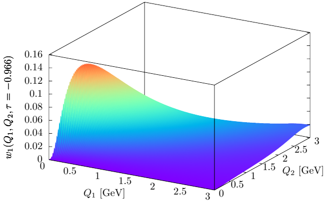

$\tau = -0.966, \quad \theta = 165^\circ$

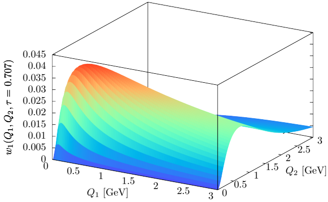

$\tau = 0.707, \quad \theta = 45^\circ$

Weight function $w_2(Q_1, Q_2, \tau)$

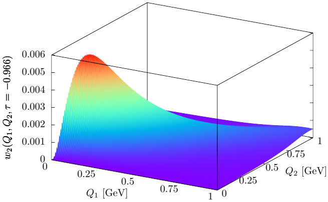

$\tau = -0.966, \quad \theta = 165^\circ$

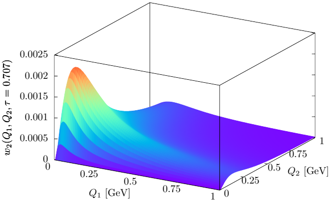

$\tau = 0.707, \quad \theta = 45^\circ$

Peaks and ridges have broadened even more compared to η.

Peak for w_1 around $Q_1 \sim 0.41 - 0.51$ GeV, $Q_2 \sim 0.31 - 0.43$ GeV.

w_2 about a factor 20 smaller than w_1. Peak for w_2 around $Q_1 = Q_2 \sim 0.14$ GeV for τ near -1, moves down to $Q_1 = Q_2 = 0.07$ GeV for τ near 1.

w_2: finite result for constant form factor $\left(\frac{\alpha}{\pi}\right)^3 a_{\mu;\mathrm{WZW}}^{\mathrm{HLbL};\eta'(2)} = 0.65 \times 10^{-11}$

Relevant momentum regions in $a_\mu^{\mathrm{HLbL;P}}$

For illustration: LMD+V and VMD models

- Since integral $a_\mu^{\mathrm{HLbL};\pi^0(1)}$ is divergent without form factors, we take two simple models for illustration to see where are the relevant momentum regions in the integral.
- Of course, in the end, the models have to be replaced by experimental data on the doubly-virtual form factor $\mathcal{F}_{\pi^0\gamma^*\gamma^*}(-Q_1^2, -Q_2^2)$.
- LMD+V model (Lowest Meson Dominance + V) is generalization of Vector Meson Dominance (VMD) in framework of large-N_C QCD, which respects (some) short-distance constraints from operator product expansion (OPE).
- Main difference is doubly-virtual case: VMD model violates OPE, falls off too fast:

$$\mathcal{F}_{\pi^0\gamma^*\gamma^*}^{\mathrm{VMD}}(-Q^2, -Q^2) \quad \sim \quad \frac{1}{Q^4} \qquad \text{for large } Q^2$$

$$\mathcal{F}_{\pi^0\gamma^*\gamma^*}^{\mathrm{LMD+V}}(-Q^2, -Q^2) \quad \sim \quad \mathcal{F}_{\pi^0\gamma^*\gamma^*}^{\mathrm{OPE}}(-Q^2, -Q^2) \sim \frac{1}{Q^2} \qquad \text{for large } Q^2$$

- η, η': use VMD model with adapted parameter F_{P} to describe $\Gamma(\mathrm{P} \to \gamma\gamma)$ and M_V from fit of $\mathcal{F}_{\mathrm{P}\gamma^*\gamma^*}(-Q^2, 0)$ to CLEO data.

Form factor model: LMD+V (large-N_c QCD) versus VMD

Define: $\Delta\mathcal{F}(Q_1^2, Q_2^2) = \mathcal{F}^{\mathrm{LMD+V}}_{\pi^0\gamma^*\gamma^*}(-Q_1^2, -Q_2^2) - \mathcal{F}^{\mathrm{VMD}}_{\pi^0\gamma^*\gamma^*}(-Q_1^2, -Q_2^2)$

$$\frac{\mathcal{F}^{\mathrm{LMD+V}}_{\pi^0\gamma^*\gamma^*}(-Q_1^2,-Q_2^2)}{\mathcal{F}_{\pi^0\gamma^*\gamma^*}(0,0)}$$

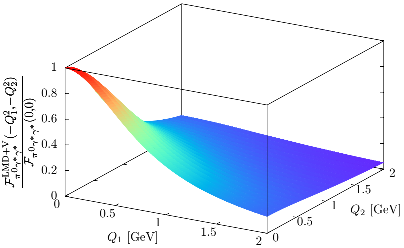

$$\frac{\Delta\mathcal{F}(Q_1^2,Q_2^2)}{\mathcal{F}^{\mathrm{LMD+V}}_{\pi^0\gamma^*\gamma^*}(-Q_1^2,-Q_2^2)}$$

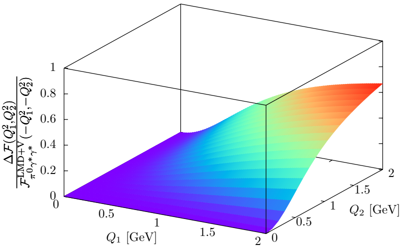

Q_1 [GeV]	Q_2 [GeV]	$\frac{\mathcal{F}^{\mathrm{LMD+V}}_{\pi^0\gamma^*\gamma^*}(-Q_1^2,-Q_2^2)}{\mathcal{F}_{\pi^0\gamma^*\gamma^*}(0,0)}$	$\frac{\mathcal{F}^{\mathrm{VMD}}_{\pi^0\gamma^*\gamma^*}(-Q_1^2,-Q_2^2)}{\mathcal{F}_{\pi^0\gamma^*\gamma^*}(0,0)}$	$\frac{\Delta\mathcal{F}(Q_1^2,Q_2^2)}{\mathcal{F}^{\mathrm{LMD+V}}_{\pi^0\gamma^*\gamma^*}(-Q_1^2,-Q_2^2)}$
0.5	0	0.707	0.706	0.0003
1	0	0.376	0.376	0.001
0.5	0.5	0.513	0.499	0.027
1	1	0.183	0.141	0.23

For single-virtual FF, both models give equally good fit to CLEO data. Main difference: double-virtual case.

Since LMD+V and VMD FF differ for $Q_1 = Q_2 = 1$ GeV by 23%, it might be possible to distinguish the two models experimentally at BESIII, if binning is chosen properly.

Contributions to $a_\mu^{\mathrm{HLbL};\pi^0}$ from different momentum regions

$$a_{\mu;\mathrm{LMD+V}}^{\mathrm{HLbL};\pi^0} = 62.9 \times 10^{-11}$$
$$a_{\mu;\mathrm{VMD}}^{\mathrm{HLbL};\pi^0} = 57.0 \times 10^{-11}$$

Integrate over momentum bins:

$$\int_{Q_{1,\min}}^{Q_{1,\max}} dQ_1 \int_{Q_{2,\min}}^{Q_{2,\max}} dQ_2 \int_{-1}^{1} d\tau$$

Contribution of individual bins to total:

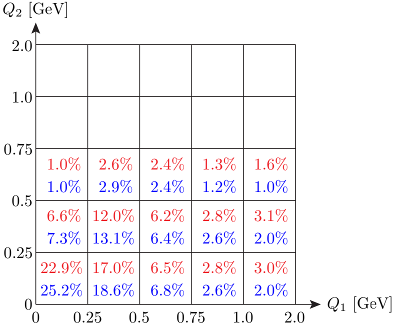

Bin sizes vary. No entry: contribution $< 1\%$.
Asymmetry in (Q_1, Q_2)-plane with larger contributions below diagonal reflects ridge-like structure in dominant $w_1(Q_1, Q_2, \tau)$.

Pion-pole contribution $a_\mu^{\mathrm{HLbL};\pi^0} \times 10^{11}$ for LMD+V and VMD form factors obtained with momentum cutoff Λ.

Λ [GeV]	LMD+V	VMD
0.25	14.4 (22.9%)	14.4 (25.2%)
0.5	36.8 (58.5%)	36.6 (64.2%)
0.75	48.5 (77.1%)	47.7 (83.8%)
1.0	54.1 (86.0%)	52.6 (92.3%)
1.5	58.8 (93.4%)	55.8 (97.8%)
2.0	60.5 (96.2%)	56.5 (99.2%)
5.0	62.5 (99.4%)	56.9 (99.9%)
20.0	62.9 (100%)	57.0 (100%)

LMD+V and VMD: almost identical absolute contributions below $\Lambda = 0.5$ GeV (0.75 GeV), form factors differ by less than 3% (10%).

Region below $\Lambda = 0.5$ GeV gives more than half of the contribution: 59% for LMD+V, 64% for VMD.

Bulk of result below $\Lambda = 1$ GeV: 86% for LMD+V, 92% for VMD.

VMD: faster fall-off at high momenta
$\Rightarrow$ overall smaller contribution compared to LMD+V.

Contributions to $a_\mu^{\mathrm{HLbL};\eta}$ and $a_\mu^{\mathrm{HLbL};\eta'}$ from different momentum regions

One obtains with VMD model:

$$a_{\mu;\mathrm{VMD}}^{\mathrm{HLbL};\eta} = 14.5 \times 10^{-11}$$

$$a_{\mu;\mathrm{VMD}}^{\mathrm{HLbL};\eta'} = 12.5 \times 10^{-11}$$

Contribution of individual bins to total (bin sizes vary; no entry: contribution $< 1\%$):

Q_2 [GeV] \ Q_1 [GeV]	0 – 0.25	0.25 – 0.5	0.5 – 0.75	0.75 – 1.0	1.0 – 2.0
1.0 – 2.0		1.4%	1.0% 1.9%	1.8%	1.6% 3.3%
0.75 – 1.0		1.7% 2.5%	1.9% 2.9%	1.4% 2.2%	1.5% 2.5%
0.5 – 0.75	2.3% 2.5%	6.2% 7.0%	5.3% 6.4%	2.7% 3.5%	2.3% 3.2%
0.25 – 0.5	8.8% 7.1%	16.6% 14.1%	8.5% 7.8%	3.5% 3.4%	2.7% 2.9%
0 – 0.25	12.1% 7.9%	10.0% 7.0%	3.7% 2.8%	1.4% 1.2%	1.1%

Pole contributions $a_\mu^{\mathrm{HLbL};\eta} \times 10^{11}$ and $a_\mu^{\mathrm{HLbL};\eta'} \times 10^{11}$ with VMD form factor obtained with momentum cutoff Λ.

Λ [GeV]	η	η'
0.25	1.8 (12.1%)	1.0 (7.9%)
0.5	6.9 (47.5%)	4.5 (36.1%)
0.75	10.7 (73.4%)	7.8 (62.5%)
1.0	12.6 (86.6%)	9.9 (79.1%)
1.5	14.0 (96.1%)	11.7 (93.1%)
2.0	14.3 (98.6%)	12.2 (97.4%)
5.0	14.5 (100%)	12.5 (99.9%)
20.0	14.5 (100%)	12.5 (100%)

Region below $\Lambda = 0.25$ GeV gives very small contribution to total: 12% for η, 8% for η'.

Region below $\Lambda = 0.5$ GeV gives: 48% for η, 36% for η'.

Bulk of result below $\Lambda = 1.5$ GeV: 96% for η, 93% for η'.

VMD model might underestimate contribution due to too fast fall-off.

Impact of form factor uncertainties on $a_\mu^{\mathrm{HLbL;P}}$

Parametrization of form factor uncertainties

Single-virtual form factor: rough description of measurement errors

$$\mathcal{F}_{\mathrm{P}\gamma^*\gamma^*}(-Q^2,0) \to \mathcal{F}_{\mathrm{P}\gamma^*\gamma^*}(-Q^2,0)\,(1+\delta_{1,\mathrm{P}}(Q))$$

where we assume the following momentum dependent errors:

Region [GeV]	$\delta_{1,\pi^0}(Q)$	$\delta_{1,\eta}(Q)$	$\delta_{1,\eta'}(Q)$
$0 \leq Q < 0.5$	5% [2%]	10%	6%
$0.5 \leq Q < 1$	7% [4%]	15%	11%
$1 \leq Q < 2$	8%	8%	7%
$2 \leq Q$	4%	4%	4%

Error estimates based on:

π^0: $\Gamma(\pi^0 \to \gamma\gamma)$ from PrimEx; TFF in spacelike region from CELLO, CLEO, BABAR, Belle, ongoing analysis by BESIII (future KLOE-2 ?)
η: $\Gamma(\eta \to \gamma\gamma)$ from KLOE-2; spacelike TFF: in addition TPC/2γ; timelike TFF from single Dalitz decays $\eta \to \ell^+\ell^-\gamma$ (NA60: $\ell = \mu$; A2: $\ell = e$)
η': $\Gamma(\eta' \to \gamma\gamma)$ from L3; spacelike TFF below 0.5 GeV from L3 (untagged); timelike TFF from $\eta \to e^+e^-\gamma$ from BESIII
π^0, η: assumed error in lowest momentum bin (no reliable data in spacelike region)
[ ]: use DR for spacelike TFF at low energies (Hoferichter et al. '14)

Parametrization of form factor uncertainties (continued)

Double-virtual form factor: description of measurement errors

$$\mathcal{F}_{\mathrm{P}\gamma^*\gamma^*}(-Q_1^2, -Q_2^2) \to \mathcal{F}_{\mathrm{P}\gamma^*\gamma^*}(-Q_1^2, -Q_2^2)\,(1 + \delta_{2,\mathrm{P}}(Q_1, Q_2))$$

$\mathcal{F}_{\mathrm{P}\gamma^*\gamma^*}(-Q_1^2, -Q_2^2)$: no experimental data yet.

Measurement planned at BESIII.

Estimate error with Monte Carlo simulations by Mainz group (Denig, Redmer, Wasser) for $e^+e^- \to e^+e^-\gamma^*\gamma^* \to e^+e^-\mathrm{P}$ at BESIII (signal process only !) with EKHARA (Czyż, Ivashyn '11; Czyż et al. '12).

LMD+V model for π^0, VMD model for η, η'.

Uncertainties of double-virtual form factor from Monte Carlo

$\delta_{2,\pi^0}(Q_1, Q_2)$

Q_2 [GeV] \ Q_1 [GeV]	0 – 0.5	0.5 – 0.75	0.75 – 1.0	1.0 – 2.0
1.0 – 2.0	9% (31)	8% (42)	10% (23)	11% (20)
0.75 – 1.0	8% (42)	6% (62)	8% (35)	10% (23)
0.5 – 0.75	9% (32)	5% (86)	6% (62)	8% (42)
0 – 0.5	8%	9% (32)	8% (42)	9% (31)

Note unequal bin sizes !
In brackets: number of MC events N_i in each bin $\sim \sigma \sim \mathcal{F}^2_{\pi^0\gamma^*\gamma^*} \Rightarrow \delta\mathcal{F}_{\pi^0\gamma^*\gamma^*} = \sqrt{N_i}/(2N_i)$ (total: 600 events).
Lowest bin: assumed error.
"Extrapolation" from boundary values (average of neighboring bins), no events in simulation (detector acceptance).

$\delta_{2,\eta}(Q_1, Q_2), \delta_{2,\eta'}(Q_1, Q_2)$

Q_2 [GeV] \ Q_1 [GeV]	0 – 0.5	0.5 – 0.75	0.75 – 1.0	1.0 – 2.0
1.0 – 2.0	11% / 7%	12% / 7%	18% / 10%	25% / 13%
0.75 – 1.0	9% / 6%	9% / 6%	13% / 8%	18% / 10%
0.5 – 0.75	10% / 6%	7% / 4%	9% / 6%	12% / 7%
0 – 0.5	9% / 5%	10% / 6%	9% / 6%	11% / 7%

Top line in bin: η-meson (345 events).
Bottom line: η'-meson (902 events).
Lowest bin: assumed error.

Number of events and corresponding precision for $\mathcal{F}_{\mathrm{P}\gamma^*\gamma^*}(-Q_1^2, -Q_2^2)$ should be achievable with current data set at BESIII plus a few more years of data taking. Separation of signal and background will be more difficult for η and η' than for π^0.

Impact of form factor uncertainties on $a_{\mu}^{\mathrm{HLbL;P}}$

With the given errors $\delta_{1,\mathrm{P}}(Q)$ and $\delta_{2,\mathrm{P}}(Q_1, Q_2)$ we obtain:

$$
\begin{aligned}
a_{\mu;\mathrm{LMD+V}}^{\mathrm{HLbL};\pi^0} &= 62.9^{+8.9}_{-8.2} \times 10^{-11} \quad \binom{+14.1\%}{-13.1\%} \\
a_{\mu;\mathrm{VMD}}^{\mathrm{HLbL};\pi^0} &= 57.0^{+7.8}_{-7.3} \times 10^{-11} \quad \binom{+13.7\%}{-12.7\%} \\
a_{\mu;\mathrm{VMD}}^{\mathrm{HLbL};\eta} &= 14.5^{+3.4}_{-3.0} \times 10^{-11} \quad \binom{+23.4\%}{-20.8\%} \\
a_{\mu;\mathrm{VMD}}^{\mathrm{HLbL};\eta'} &= 12.5^{+1.9}_{-1.7} \times 10^{-11} \quad \binom{+15.1\%}{-13.9\%}
\end{aligned}
$$

π^0: LMD+V and VMD model yield very similar relative errors. Assume that observations depend little on the used models.

Recall model calculations:

$$
\begin{aligned}
a_{\mu}^{\mathrm{HLbL};\pi^0} &= (50 - 80) \times 10^{-11} = (65 \pm 15) \times 10^{-11} \ (\pm 23\%) \\
a_{\mu}^{\mathrm{HLbL;P}} &= (59 - 114) \times 10^{-11} = (87 \pm 27) \times 10^{-11} \ (\pm 31\%)
\end{aligned}
$$

More information on single- and double-virtual TFF for π^0, η, η' in spacelike region below 1 GeV from dispersive approach and Lattice QCD ?

Impact of form factor uncertainties on $a_\mu^{\mathrm{HLbL;P}}$: more details

$\frac{\delta a_{\mu;\mathrm{LMD+V}}^{\mathrm{HLbL};\pi^0}}{a_{\mu;\mathrm{LMD+V}}^{\mathrm{HLbL};\pi^0}}$	$\frac{\delta a_{\mu;\mathrm{VMD}}^{\mathrm{HLbL};\pi^0}}{a_{\mu;\mathrm{VMD}}^{\mathrm{HLbL};\pi^0}}$	$\frac{\delta a_{\mu;\mathrm{VMD}}^{\mathrm{HLbL};\eta}}{a_{\mu;\mathrm{VMD}}^{\mathrm{HLbL};\eta}}$	$\frac{\delta a_{\mu;\mathrm{VMD}}^{\mathrm{HLbL};\eta'}}{a_{\mu;\mathrm{VMD}}^{\mathrm{HLbL};\eta'}}$	Comment
+14.1% −13.1%	+13.7% −12.7%	+23.4% −20.8%	+15.1% −13.9%	Given δ_1, δ_2
+4.3% −4.2%	+4.4% −4.3%	+6.9% −6.8%	+3.4% −3.3%	Bin $Q < 0.5$ GeV in δ_1 as given, rest: $\delta_{1,2} = 0$
+1.1% −1.0%	+1.0% −0.9%	+4.4% −4.3%	+4.5% −4.4%	Bins $Q \geq 0.5$ GeV in δ_1 as given, rest: $\delta_{1,2} = 0$
+4.5% −4.4%	+4.9% −4.8%	+4.0% −4.0%	+1.7% −1.7%	Bin $Q_{1,2} < 0.5$ GeV in δ_2 as given, rest: $\delta_{1,2} = 0$
+3.9% −3.8%	+3.2% −3.1%	+7.0% −6.8%	+5.1% −5.0%	Bins $Q_{1,2} \geq 0.5$ GeV in δ_2 as given, rest: $\delta_{1,2} = 0$
+10.9% −10.5%	+10.6% −10.1%	–	–	Given δ_1, δ_2, lowest two bins in δ_{1,π^0}: 2%, 4% [DR]
–	–	+20.4% −18.5%	–	Given δ_1, δ_2, lowest two bins in $\delta_{1,\eta}$: 8%, 10%
–	–	–	+13.4% −12.5%	Given δ_1, δ_2, lowest two bins in $\delta_{1,\eta'}$: 5%, 8%
+12.4% −11.6%	+11.8% −11.0%	+22.4% −20.0%	+14.8% −13.6%	π^0, η, η': given δ_1, δ_2, lowest bin δ_2: 5%, 7%, 4%
+12.0% −11.2%	+11.4% −10.6%	+21.9% −19.6%	+14.4% −13.4%	In addition, bins in δ_2 close to lowest: 5%, 7%, 4%

Largest error in red, second largest error in blue.

π^0: for LMD+V FF [VMD FF], region $Q_{1,2} < 0.5$ GeV gives 59% [64%] to total.

For η [η'], region $Q_{1,2} < 0.5$ GeV gives 48% [36%] to total (VMD FF).

$a_\mu^{\mathrm{HLbL};\pi^0}$: to reach goal of 10% error, it would help, if one could measure single- and double-virtual TFF in region $Q, Q_{1,2} < 0.5$ GeV. Assumed error δ_1, δ_2 in lowest bin !

$a_\mu^{\mathrm{HLbL};\eta}, a_\mu^{\mathrm{HLbL};\eta'}$: information for $0.5 \leq Q, Q_{1,2} \leq 1.5$ GeV would be very helpful !

Conclusions and Outlook

- Relevant momentum regions in $a_\mu^{\mathrm{HLbL;P}}$ from model-independent weight functions $w_{1,2}(Q_1, Q_2, \tau)$:
  - π^0: < 1 GeV
  - η and η': < 1.5 GeV

- Impact of measurement errors at BESIII of doubly-virtual form factor $\mathcal{F}_{\mathrm{P}\gamma^*\gamma^*}(-Q_1^2, -Q_2^2)$ on $a_\mu^{\mathrm{HLbL;P}}$ based on Monte Carlo simulations for

$$e^+e^- \to e^+e^-\gamma^*\gamma^* \to e^+e^-\mathrm{P}$$

  (reachable in a few more years of data taking and with other assumed input on TFF's at $Q, Q_{1,2} \leq 0.5$ GeV):

$$\begin{aligned} \delta a_\mu^{\mathrm{HLbL};\pi^0} / a_\mu^{\mathrm{HLbL};\pi^0} &= 14\% \quad [11\%] \\ \delta a_\mu^{\mathrm{HLbL};\eta} / a_\mu^{\mathrm{HLbL};\eta} &= 23\% \\ \delta a_\mu^{\mathrm{HLbL};\eta'} / a_\mu^{\mathrm{HLbL};\eta'} &= 15\% \end{aligned}$$

  [ ]: with dispersion relation (DR) for single-virtual $\mathcal{F}_{\pi^0\gamma^*\gamma^*}(-Q^2, 0)$

- In order for dispersive approach to HLbL to be successful, one needs PS-pole contributions to 10% precision $\Rightarrow$ needs to improve uncertainties !

- Future: more work needed to estimate effect of backgrounds and analysis cuts at BESIII. Further informations needed for form factors $\mathcal{F}_{\mathrm{P}\gamma^*\gamma^*}(-Q_1^2, -Q_2^2)$, in particular for low $Q_{1,2} \leq 1$ GeV, from other experiments (KLOE-2 ? Belle 2 ? CMD-3 ? SND ? Others ?), from DR for form factors and from Lattice QCD.

Backup slides

HLbL scattering: Summary of selected results for $a_\mu^{\mathrm{HLbL}} \times 10^{11}$

Contribution	BPP	HKS, HK	KN	MV	BP, MdRR	PdRV	N, JN
π^0, η, η'	85±13	82.7±6.4	83±12	114±10	–	114±13	99 ± 16
axial vectors	2.5±1.0	1.7±1.7	–	22±5	–	15±10	22±5
scalars	−6.8±2.0	–	–	–	–	−7±7	−7±2
π, K loops	−19±13	−4.5±8.1	–	–	–	−19±19	−19±13
π, K loops +subl. N_C	–	–	–	0±10	–	–	–
quark loops	21±3	9.7±11.1	–	–	–	2.3 (c-quark)	21±3
Total	83±32	89.6±15.4	80±40	136±25	110±40	105 ± 26	116 ± 39

BPP = Bijnens, Pallante, Prades '95, '96, '02; HKS = Hayakawa, Kinoshita, Sanda '95, '96; HK = Hayakawa, Kinoshita '98, '02; KN = Knecht, AN '02; MV = Melnikov, Vainshtein '04; BP = Bijnens, Prades '07; MdRR = Miller, de Rafael, Roberts '07; PdRV = Prades, de Rafael, Vainshtein '09; N = AN '09, JN = Jegerlehner, AN '09

- Pseudoscalar-exchanges dominate numerically. Other contributions not negligible. Cancellation between π, K-loops and quark loops !
- Note that recent reevaluations of axial vector contribution lead to much smaller estimates than in MV: $a_\mu^{\mathrm{HLbL;axial}} = (8 \pm 3) \times 10^{-11}$ (Pauk, Vanderhaeghen '14; Jegerlehner '14, '15). This would shift central values of compilations downwards: $a_\mu^{\mathrm{HLbL}} = (98 \pm 26) \times 10^{-11}$ (PdRV) and $a_\mu^{\mathrm{HLbL}} = (102 \pm 39) \times 10^{-11}$ (N, JN).
- PdRV: Analyzed results obtained by different groups with various models and suggested new estimates for some contributions (shifted central values, enlarged errors). Do not consider dressed light quark loops as separate contribution. Added all errors in quadrature !
- N, JN: New evaluation of pseudoscalar exchange contribution imposing new short-distance constraint on off-shell form factors. Took over most values from BPP, except axial vectors from MV. Added all errors linearly.

Expressions for weight functions $w_{1,2}(Q_1, Q_2, \tau)$

Jegerlehner, AN '09

$$w_1(Q_1, Q_2, \tau) = \left(-\frac{2\pi}{3}\right) \sqrt{1-\tau^2}\, \frac{Q_1^3 Q_2^3}{Q_2^2 + m_\pi^2}\, I_1(Q_1, Q_2, \tau)$$

$$w_2(Q_1, Q_2, \tau) = \left(-\frac{2\pi}{3}\right) \sqrt{1-\tau^2}\, \frac{Q_1^3 Q_2^3}{Q_3^2 + m_\pi^2}\, I_2(Q_1, Q_2, \tau)$$

$$\begin{aligned} I_1(Q_1, Q_2, \tau) = {} & X(Q_1, Q_2, \tau) \Big(8\, P_1\, P_2\, (Q_1 \cdot Q_2) - 2\, P_1\, P_3\, (Q_2^4/m_\mu^2 - 2\, Q_2^2) - 2\, P_1\, (2 - Q_2^2/m_\mu^2 + 2\, (Q_1 \cdot Q_2)\, /m_\mu^2) \\ & + 4\, P_2\, P_3\, Q_1^2 - 4\, P_2 - 2\, P_3\, (4 + Q_1^2/m_\mu^2 - 2\, Q_2^2/m_\mu^2) + 2/m_\mu^2 \Big) \\ & - 2\, P_1\, P_2\, (1 + (1 - R_{m1})\, (Q_1 \cdot Q_2)\, /m_\mu^2) + P_1\, P_3\, (2 - (1 - R_{m1})\, Q_2^2/m_\mu^2) + P_1\, (1 - R_{m1})/m_\mu^2 \\ & + P_2\, P_3\, (2 + (1 - R_{m1})^2\, (Q_1 \cdot Q_2)\, /m_\mu^2) + 3\, P_3\, (1 - R_{m1})/m_\mu^2 \end{aligned}$$

$$\begin{aligned} I_2(Q_1, Q_2, \tau) = {} & X(Q_1, Q_2, \tau) \Big(4\, P_1\, P_2\, (Q_1 \cdot Q_2) + 2\, P_1\, P_3\, Q_2^2 - 2\, P_1 + 2\, P_2\, P_3\, Q_1^2 - 2\, P_2 - 4 P_3 - 4/m_\mu^2 \Big) \\ & - 2\, P_1\, P_2 - 3\, P_1\, (1 - R_{m2})/(2m_\mu^2) - 3\, P_2\, (1 - R_{m1})/(2m_\mu^2) - P_3\, (2 - R_{m1} - R_{m2})/(2m_\mu^2) \\ & + P_1\, P_3\, (2 + 3\, (1 - R_{m2})\, Q_2^2/(2m_\mu^2) + (1 - R_{m2})^2\, (Q_1 \cdot Q_2)\, /(2m_\mu^2)) \\ & + P_2\, P_3\, (2 + 3\, (1 - R_{m1})\, Q_1^2/(2m_\mu^2) + (1 - R_{m1})^2\, (Q_1 \cdot Q_2)\, /(2m_\mu^2)) \end{aligned}$$

where $Q_3^2 = (Q_1 + Q_2)^2, \quad Q_1 \cdot Q_2 = Q_1 Q_2 \cos\theta, \quad \tau = \cos\theta$

$P_1^2 = 1/Q_1^2, \quad P_2^2 = 1/Q_2^2, \quad P_3^2 = 1/Q_3^2, \quad X(Q_1, Q_2, \tau) = \frac{1}{Q_1 Q_2\, x} \arctan\left(\frac{zx}{1 - z\tau}\right),$

$x = \sqrt{1-\tau^2}, \quad z = \frac{Q_1 Q_2}{4m_\mu^2}\, (1 - R_{m1})\, (1 - R_{m2}), \quad R_{mi} = \sqrt{1 + 4m_\mu^2/Q_i^2}$

Locations and values of maxima of $w_{1,2}(Q_1, Q_2, \tau)$ for π^0

θ ($\tau = \cos\theta$)	Max. w_1	Q_1 [GeV]	Q_2 [GeV]	Max. w_2	$Q_1 = Q_2$ [GeV]
175° (-0.996)	0.592	0.163	0.163	0.100	0.142
165° (-0.966)	1.734	0.164	0.162	0.277	0.132
150° (-0.866)	3.197	0.166	0.158	0.441	0.114
135° (-0.707)	4.176	0.171	0.153	0.494	0.099
120° (-0.5)	4.559	0.176	0.146	0.471	0.087
105° (-0.259)	4.349	0.182	0.139	0.403	0.078
90° (0.0)	3.664	0.187	0.130	0.312	0.070
75° (0.259)	2.702	0.189	0.122	0.218	0.063
60° (0.5)	1.691	0.187	0.114	0.132	0.057
45° (0.707)	0.840	0.180	0.106	0.064	0.050
30° (0.866)	0.283	0.168	0.099	0.021	0.043
15° (0.966)	0.0385	0.154	0.092	0.0027	0.037
5° (0.996)	0.0015	0.147	0.089	0.000092	0.037

- Global maximum of $w_1(Q_1, Q_2, \tau) = 4.563$
  ($Q_1 = 0.177$ GeV, $Q_2 = 0.145$ GeV, $\theta = 118.1^\circ$ ($\tau = -0.471$))
- Global minimum of $w_1(Q_1, Q_2, \tau) = -0.0044$
  ($Q_1 = 0.118$ GeV, $Q_2 = 1.207$ GeV, $\theta = 45.7^\circ$ ($\tau = 0.698$))
- Global maximum of $w_2(Q_1, Q_2, \tau) = 0.495$
  ($Q_1 = Q_2 = 0.097$ GeV and $\theta = 133.1^\circ$ ($\tau = -0.684$))

Locations of maxima of $w_{1,2}(Q_1, Q_2, \tau)$ for η (top) and η' (bottom)

θ ($\tau = \cos\theta$)	Max. w_1	Q_1 [GeV]	Q_2 [GeV]	Max. w_2	$Q_1 = Q_2$ [GeV]
175° (-0.996)	0.117	0.328	0.328	0.0061	0.143
165° (-0.966)	0.341	0.327	0.327	0.018	0.142
150° (-0.866)	0.616	0.325	0.323	0.032	0.137
135° (-0.707)	0.778	0.323	0.317	0.041	0.131
120° (-0.5)	0.809	0.322	0.308	0.044	0.123
105° (-0.259)	0.729	0.323	0.296	0.040	0.114
90° (0.0)	0.575	0.328	0.282	0.032	0.106
75° (0.259)	0.395	0.336	0.267	0.023	0.096
60° (0.5)	0.231	0.346	0.253	0.014	0.087
45° (0.707)	0.107	0.356	0.241	0.0063	0.077
30° (0.866)	0.034	0.363	0.231	0.0019	0.067
15° (0.966)	0.0044	0.367	0.225	0.00023	0.063
5° (0.996)	0.00017	0.368	0.224	8×10^{-6}	0.065
175° (-0.996)	0.049	0.434	0.434	0.0020	0.143
165° (-0.966)	0.142	0.432	0.433	0.0059	0.142
150° (-0.866)	0.255	0.427	0.430	0.011	0.139
135° (-0.707)	0.320	0.419	0.423	0.014	0.134
120° (-0.5)	0.330	0.413	0.412	0.015	0.128
105° (-0.259)	0.293	0.412	0.397	0.014	0.120
90° (0.0)	0.227	0.418	0.378	0.011	0.112
75° (0.259)	0.154	0.431	0.358	0.0079	0.102
60° (0.5)	0.088	0.451	0.340	0.0047	0.092
45° (0.707)	0.041	0.472	0.326	0.0022	0.082
30° (0.866)	0.013	0.491	0.315	0.00066	0.072
15° (0.966)	0.0017	0.504	0.309	0.000079	0.067
5° (0.996)	0.000062	0.508	0.307	3×10^{-6}	0.070

Form factor $\mathcal{F}_{\pi^0\gamma^*\gamma^*}(q_1^2, q_2^2)$ and transition form factor $F(Q^2)$

- Form factor $\mathcal{F}_{\pi^0\gamma^*\gamma^*}(q_1^2, q_2^2)$ between an on-shell pion and two off-shell (virtual) photons:

$$i \int d^4x\, e^{iq_1 \cdot x} \langle 0 | T\{j_\mu(x) j_\nu(0)\} | \pi^0(q_1 + q_2) \rangle = \varepsilon_{\mu\nu\alpha\beta}\, q_1^\alpha\, q_2^\beta\, \mathcal{F}_{\pi^0\gamma^*\gamma^*}(q_1^2, q_2^2)$$

$$j_\mu(x) = (\overline{\psi} \hat{Q} \gamma_\mu \psi)(x), \quad \psi \equiv \begin{pmatrix} u \\ d \\ s \end{pmatrix}, \quad \hat{Q} = \mathrm{diag}(2, -1, -1)/3$$

(light quark part of electromagnetic current)

Bose symmetry: $\mathcal{F}_{\pi^0\gamma^*\gamma^*}(q_1^2, q_2^2) = \mathcal{F}_{\pi^0\gamma^*\gamma^*}(q_2^2, q_1^2)$

Form factor for real photons is related to $\pi^0 \to \gamma\gamma$ decay width:

$$\mathcal{F}^2_{\pi^0\gamma^*\gamma^*}(q_1^2 = 0, q_2^2 = 0) = \frac{4}{\pi\alpha^2 m_\pi^3} \Gamma_{\pi^0 \to \gamma\gamma}$$

Often normalization with chiral anomaly is used:

$$\mathcal{F}_{\pi^0\gamma^*\gamma^*}(0, 0) = -\frac{1}{4\pi^2 F_\pi}$$

- Pion-photon transition form factor:

$$F(Q^2) \equiv \mathcal{F}_{\pi^0\gamma^*\gamma^*}(-Q^2, q_2^2 = 0), \qquad Q^2 \equiv -q_1^2$$

Note that $q_2^2 = 0$, but $\vec{q}_2 \neq \vec{0}$ for on-shell photon !

The LMD+V form factor

Knecht, AN, EPJC '01; AN '09

- Ansatz for $\langle VVP \rangle$ and thus $\mathcal{F}_{\pi^0\gamma^*\gamma^*}$ in large-N_c QCD in chiral limit with 1 multiplet of lightest pseudoscalars (Goldstone bosons) and 2 multiplets of vector resonances, ρ, ρ' (lowest meson dominance (LMD) + V).
- $\mathcal{F}_{\pi^0\gamma^*\gamma^*}$ fulfills all leading and some subleading QCD short-distance constraints from operator product expansion (OPE).
- Reproduces Brodsky-Lepage (BL): $\lim_{Q^2\to\infty} \mathcal{F}_{\pi^0\gamma^*\gamma^*}(-Q^2, 0) \sim 1/Q^2$

  (OPE and BL cannot be fulfilled simultaneously with only one vector resonance).
- Normalized to decay width $\Gamma_{\pi^0\to\gamma\gamma}$

$$\mathcal{F}^{\mathrm{LMD+V}}_{\pi^0\gamma^*\gamma^*}(q_1^2, q_2^2) = \frac{F_\pi}{3} \frac{q_1^2\, q_2^2\, (q_1^2 + q_2^2) + h_1\, (q_1^2 + q_2^2)^2 + \bar{h}_2\, q_1^2\, q_2^2 + \bar{h}_5\, (q_1^2 + q_2^2) + \bar{h}_7}{(q_1^2 - M_{V_1}^2)\, (q_1^2 - M_{V_2}^2)\, (q_2^2 - M_{V_1}^2)\, (q_2^2 - M_{V_2}^2)}$$

$F_\pi = 92.4$ MeV, $M_{V_1} = M_\rho = 775.49$ MeV, $M_{V_2} = M_{\rho'} = 1465$ MeV

Free model parameters: $h_i, \bar{h}_i$

Transition form factor:

$$F^{\mathrm{LMD+V}}(Q^2) = \frac{F_\pi}{3} \frac{1}{M_{V_1}^2 M_{V_2}^2} \frac{h_1\, Q^4 - \bar{h}_5\, Q^2 + \bar{h}_7}{(Q^2 + M_{V_1}^2)(Q^2 + M_{V_2}^2)}$$

- $h_1 = 0$ GeV^2 (Brodsky-Lepage behavior $\mathcal{F}^{\mathrm{LMD+V}}_{\pi^0\gamma^*\gamma}(-Q^2, 0) \sim 1/Q^2$)
- $\bar{h}_2 = -10.63$ GeV^2 (Melnikov, Vainshtein '04: Higher twist corrections in OPE)
- $\bar{h}_5 = 6.93 \pm 0.26$ GeV$^4 - h_3 m_\pi^2$ (fit to CLEO data of $\mathcal{F}^{\mathrm{LMD+V}}_{\pi^0\gamma^*\gamma}(-Q^2, 0)$)
- $\bar{h}_7 = -\frac{N_c M_{V_1}^4 M_{V_2}^4}{4\pi^2 F_\pi^2} = -14.83$ GeV^6 (or normalization to $\Gamma(\pi^0 \to \gamma\gamma)$)

The VMD form factor

Vector Meson Dominance:

$$\mathcal{F}^{\mathrm{VMD}}_{\pi^{0*}\gamma^*\gamma^*}(q_1^2, q_2^2) = -\frac{N_c}{12\pi^2 F_\pi} \frac{M_V^2}{q_1^2 - M_V^2} \frac{M_V^2}{q_2^2 - M_V^2}$$

Only two model parameters: F_π and M_V.

Note:

- VMD form factor factorizes $\mathcal{F}^{\mathrm{VMD}}_{\pi^0\gamma^*\gamma^*}(q_1^2, q_2^2) = f(q_1^2) \times f(q_2^2)$. This might be a too simplifying assumption / representation.
- VMD form factor has wrong short-distance behavior: $\mathcal{F}^{\mathrm{VMD}}_{\pi^0\gamma^*\gamma^*}(q^2, q^2) \sim 1/q^4$, for large q^2, falls off too fast compared to OPE prediction $\mathcal{F}^{\mathrm{OPE}}_{\pi^0\gamma^*\gamma^*}(q^2, q^2) \sim 1/q^2$.

Transition form factor:

$$F^{\mathrm{VMD}}(Q^2) = -\frac{N_c}{12\pi^2 F_\pi} \frac{M_V^2}{Q^2 + M_V^2}$$

For numerics:

$$\begin{aligned} F_\pi &= 92.4 \text{ MeV}, \quad M_V = M_\rho = 775.49 \text{ MeV} \\ F_\eta &= 93.0 \text{ MeV}, \quad M_V = 775 \text{ MeV} \\ F_{\eta'} &= 74.0 \text{ MeV}, \quad M_V = 859 \text{ MeV} \end{aligned}$$

η, η': F_{P} to describe $\Gamma(\mathrm{P} \to \gamma\gamma)$ and M_V from fit of $\mathcal{F}_{\mathrm{P}\gamma^*\gamma^*}(-Q^2, 0)$ to CLEO data.